Longitudinal spin asymmetries and ΔG at COMPASS

Jean-Marc Le Goff, on behalf of COMPASS collaboration

CEA-Saclay, DAPNIA, 91191 Gif-sur-Yvette

E-mail: jmlegoff@cea.fr

Abstract. The spin structure g_1 of the deuteron has been measured by COMPASS with unprecedented accuracy at low x, providing much more reliable values for the first moment Γ_1 and for the quark spin contribution $\Delta\Sigma$. Difference-charge semi-inclusive asymmetries have been measured and seem to favor a flavor asymmetric polarized sea. The gluon polarization has been measured in the open-charm and high-p_t channels. Large values of ΔG are now unlikely.

1. Introduction

The spin $\frac{1}{2}$ of the nucleon can be decomposed in the contributions from its constituents as $\frac{1}{2} = \frac{1}{2}\Delta\Sigma + \Delta G + L_z$, where the three contributions come from quark spins, gluon spins and orbital momentum, respectively. The quark contribution can be further decomposed in terms of sea and valence and the different flavors as $\Delta\Sigma = \Delta u_v + \Delta d_v + 2\Delta\bar{u} + 2\Delta\bar{d} + \Delta s + \Delta\bar{s}$. Here, we will present studies of $\Delta\Sigma$, $\Delta u_v + \Delta d_v$ and ΔG at COMPASS.

2. The COMPASS experiment

The COMPASS experiment includes about 240 physicists from 25 institutes. It makes use of either a polarized muon beam or hadron beams. Studies with hadron beams include Primakov reactions (with the aim of measuring the π and K polarizabilities), searches for exotic quark states and glueballs and searches for double-charmed hadrons. In addition to the studies presented here, the muon beam is used to measure transversity and the production of ρ, Φ, J/Ψ, Λ, ...

The M2 beam line at CERN provides $2 \cdot 10^8$ μ per 4.8 s spill every 16.8 s. The 160 GeV muons with -80% polarization impinge on a deuteron target (^{6}LiD) polarized to 50%, providing a luminosity of $5 \cdot 10^{32}$ cm^{-2}s^{-1}. The resulting particles are tracked and identified in a two-stage spectrometer [1]. The first spectrometer detects large-angle small-momentum particles and is equipped with a RICH detector for K identification.

The polarized target is equipped with two cells polarized oppositely, which are exposed to the same μ beam. The direction of the spins in the two cells are inverted every 8 hours by rotating the target magnetic field. The measured counting-rate asymmetry is $\frac{N_u - N_d}{N_u + N_d} = (f P_T P_\mu D) A_1 + A_{acpt}$, where A_1 is the physical asymmetry and A_{acpt} is the asymmetry due to the fact that the two cells are seen by the spectrometer with a different acceptance. After inverting the spin direction we have $\frac{N'_u - N'_d}{N'_u + N'_d} = -(f P_T P_\mu D) A_1 + A_{acpt}$. If the acceptance is stable A_{acpt} cancels out in the difference between the two counting-rate asymmetries which then provides the physical asymmetry A_1; spectrometer instabilities may prevent a perfect cancellation of A_{acpt} and result in "false asymmetries". To get a statistically optimal result, each event is given an individual

weight corresponding to its sensitivity to A_1, $w = fP_\mu D$. This results in a gain in the statistical factor of merit of $1 + \sigma_w^2/\overline{w}^2$.

3. Inclusive analysis

The inclusive asymmetries, $\mu d \to \mu' X$, measured at COMPASS for $Q^2 > 1$ GeV^2 [2] are presented in Fig. 1. They are compatible with previous measurements but represent a factor 3 to 4 gain in statistics at low x. They are compatible with zero at small x, which does not confirm the trend for negative values observed previously. The measured asymmetries are used to compute the spin structure function of the deuteron $g_1^d = A_1^d F_2^d / 2x(1+R)$.

As can be seen on Fig. 2 the new g_1^d data are not compatible at low x with previous QCD fits. A new next-to-leading order QCD analysis of world data was then performed [2] including these new data. This analysis results in two possible solutions with comparable χ^2 as shown on Fig. 2, one with $\Delta G > 0$ and one with $\Delta G < 0$. In both cases $|\Delta G| \approx 02 - 0.3$.

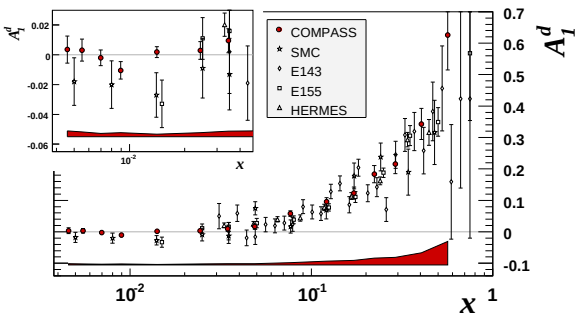

Figure 1. The inclusive spin asymmetry A_1^d measured at $Q^2 > 1$ GeV^2 by COMPASS [2] SMC [3], HERMES [4], E143 [5] and E155 [6]. The shaded band indicates COMPASS systematic errors. The insert demonstrates the gain in statistics at low x.

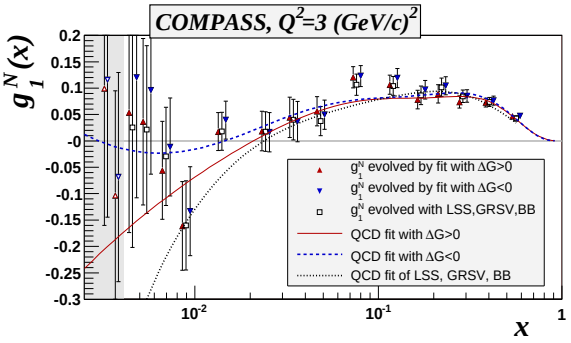

Figure 2. NLO QCD analysis of g_1 world data. Previous analyses (·····) are not compatible with the new data at low x. The new analysis provides two solutions with either $\Delta G > 0$ (——) or $\Delta G < 0$ (- - - -).

The dominant error in the first moment, $\Gamma_1^d = \int_0^1 g_1(x)dx$, used to be the contribution from the unmeasured low x region. Previous QCD fits were giving large negative values at low x, resulting in a 50% negative correction to Γ_1^d. With the new data the low x extrapolation is much more constrained and, in addition, the low x correction is only 2% of Γ_1^d. This now provides a robust measurement of the axial matrix element $a_0 = 0.30 \pm 0.01(stat) \pm 0.02(syst)$. In the absence of the axial anomaly this gives a quark contribution to the nucleon spin $\Delta\Sigma = a_0$.

4. Semi-inclusive analysis

In leading order QCD the semi-inclusive asymmetry, $\mu d \to \mu' h X$, can be written as $A^h = \dfrac{\sum e_q^2 \Delta q(x) D_q^h(z)}{\sum e_q^2 q(x) D_q^h(z)}$. The fragmentation function D_q^h of quark q in a hadron h with a fraction z of the quark momentum differs for quarks and anti-quarks. Semi-inclusive asymmetries then allow for a separation of quark and antiquark or rather valence and sea contributions. The asymmetries measured at COMPASS for positive- and negative-charge hadrons are presented in Fig. 3 and 4, respectively. The data are compatible with previous ones. At large x the error bars are similar to those of HERMES, at low x only SMC had data before and the new data provide much smaller errors.

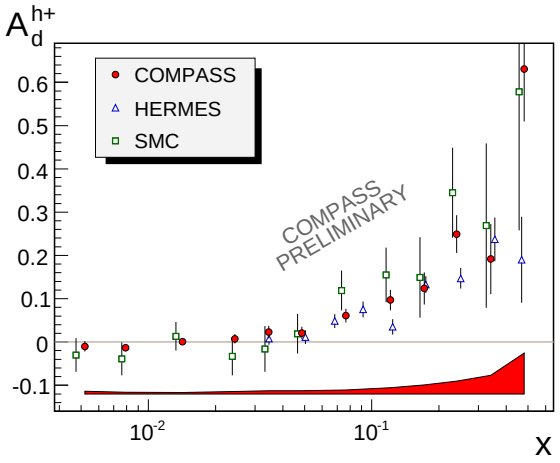

Figure 3. Semi-inclusive asymmetries measured by COMPASS [7], SMC [8] and HERMES [4] for positive-charge hadrons. The lower band indicates the COMPASS systematic errors.

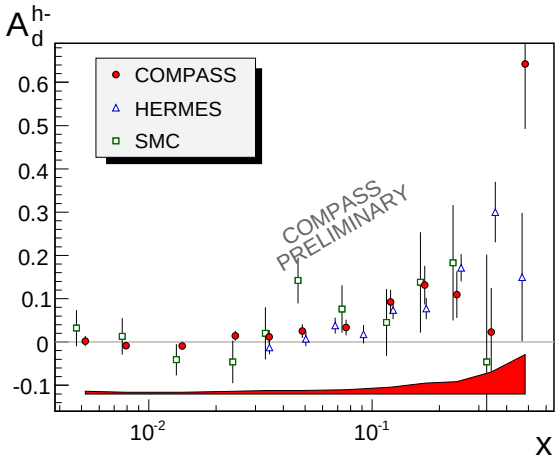

Figure 4. Semi-inclusive asymmetries measured by COMPASS [7], SMC [8] and HERMES [4] for negative-charge hadrons. The lower band indicates the COMPASS systematic errors.

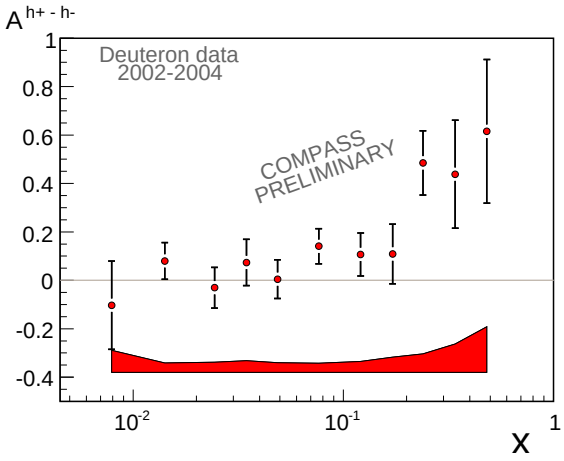

Figure 5. Difference-charge asymmetry measured at COMPASS [7]. The lower band indicates systematic errors.

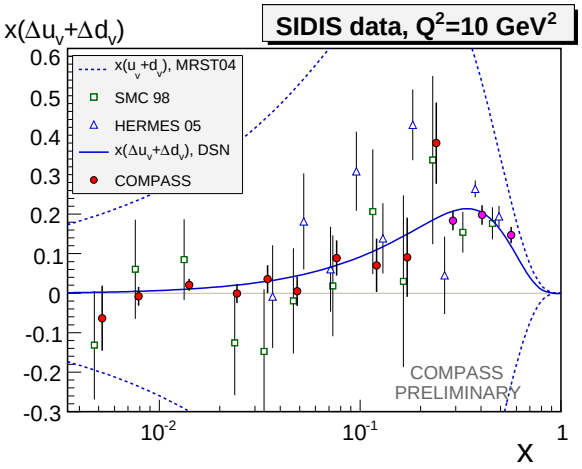

Figure 6. The polarized valence quark distribution $x(\Delta u_v(x)+\Delta d_v(x))$ measured at COMPASS [7], SMC [8] and HERMES [4]. The curves indicate the unpolarized valence quark distribution ($\cdots\cdots$) and the result from a fit [9] to polarized data (——).

It is interesting to consider the so-called difference-charge asymmetry, which is the spin asymmetry in the difference between the cross section for production of positive- and negative-charge hadrons. At leading order the fragmentation functions cancel out in this asymmetry, and in the case of the deuteron it involves only valence contributions : $A^{h^+-h^-} = \dfrac{\Delta u_v(x)+\Delta d_v(x)}{u_v(x)+d_v(x)}$. In practice this asymmetry is obtained from the positive- and negative-charge hadron asymmetries as $A^{h^+-h^-} = \left(A^{h^+} - rA^{h^-}\right)/(1-r)$, where r is the ratio of negative- to

positive-charge hadron cross-sections. This ratio is obtained from the ratio of the number of events, corrected by the ratio of acceptance $r = \frac{N^-}{N^+} \times \frac{a^+}{a^-}$. The acceptance correction is obtained by a MC simulation, it is very close to 1 but for the 2 or 3 highest x bins and reaches on the order of 10% in the highest x bin. Fig. 5 presents the resulting measured asymmetries [7].

These asymmetries result in the polarized valence quark distribution presented in Fig. 6. Note, however, that for the three highest x bins ($x > 0.3$) the sea is negligible with respect to the valence and $\Delta u_v(x) + \Delta d_v(x)$ has been obtained directly from $g_1^d(x)$ without using semi-inclusive data. At high x the new data have similar error bars as HERMES data while at low x they have much smaller error bars than SMC data.

The integral over x gives a total valence contribution to the nucleon spin, $\Delta u_v + \Delta d_v = 0.41 \pm 0.07 \pm 0.05$. This is two standard deviations below the value obtained in the assumption of a flavor symmetric sea ($\Delta\bar{u} = \Delta\bar{d} = \Delta s = \Delta\bar{s}$), i.e. $\Delta u_v + \Delta d_v = a_8 = 0.58 \pm 0.03$. Combining our result for $\Delta u_v + \Delta d_v$ with Γ_1 and a_8 gives $\Delta\bar{u} + \Delta\bar{d} = 0.00 \pm 0.04 \pm 0.03$. The data tend to favor a new picture of the nucleon with a flavor asymmetric polarized sea, $\Delta\bar{u} \approx -\Delta\bar{d}$, and $\Delta s + \Delta\bar{s} = -0.08 \pm 0.01 \pm 0.02$, as obtained from inclusive data.

5. The gluon polarization $\Delta G/G$

Using a lepton beam the gluons can be probed through the photon gluon fusion process (PGF), $\gamma^* g \to q\bar{q}$. There are two possible signatures for this process. We can consider events where the $q\bar{q}$ pair is a $c\bar{c}$ pair and select open-charm events (D^0 mesons). There is essentially no physics background but the cross section is small and the branching ratio of $D^0 \to K\pi$ is only 4%, which results in low statistics. The other possibility is to select events where a pair of hadrons is produced with a high transverse momentum p_t with respect to the virtual photon. This provides much larger statistics but there are several sources of physical backgrounds which must be subtracted using a MC event generator. In both cases there is a QCD hard scale, provided by m_c^2 or p_t^2, so that there is no need to require $Q^2 > 1$ GeV^2.

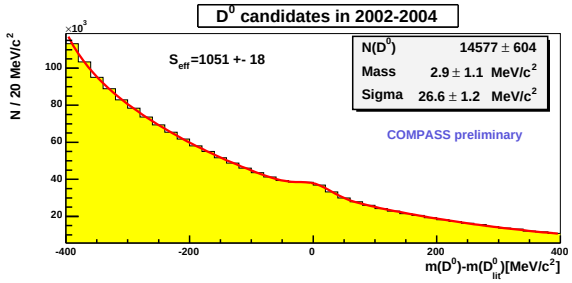

Figure 7. Reconstructed $K\pi$ masses after kinematical and RICH cuts. A small D^0 peak can be seen on a large combinatorial background.

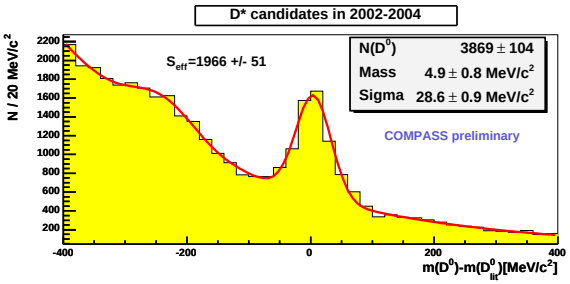

Figure 8. Same for $D^* \to D^0\pi_s$. The peak on the left is due to $D^0 \to K\pi\pi^0$ events where the π^0 is not detected.

Due to multiple scattering in the thick polarized target, it is not possible to separate the D^0 decay vertex from the primary vertex and the D^0 identification has to rely on the reconstructed $K\pi$ mass. This results in a large combinatorial background. This background is reduced by the use of the RICH detector to identify the K and by kinematical cuts $E_{D^0}/E_{\gamma^*} > 0.2$ and $|\cos\theta^*| < 0.5$, where θ^* is the K angle in the D^0 center of mass. The resulting reconstructed mass spectrum is presented in Fig. 7. Some D^0 mesons come from the decay $D^* \to D^0\pi_s$ where π_s is a slow pion. Selecting these events and cutting on $M_{K\pi\pi_s} - M_{K\pi}$ dramatically improves the signal-over-background ratio as illustrated by Fig. 8. Note that D^* candidate events are actually removed from Fig. 7 so there is no event which appears in both plots.

The counting-rate asymmetry is related to the gluon polarization by $\frac{N_u - N_d}{N_u + N_d} = f P_T P_\mu \left(a_{LL} \frac{\Delta G}{G} + A_{bckg} \right)$, where a_{LL} is the partonic asymmetry of the $\mu g \to \mu' c\bar{c}$ process and the background asymmetry is measured outside the D^0 peak. To be statistically optimal the event weight must be $w = f P_\mu a_{LL}$. However, only one D^0 is measured, so the partonic kinematics and a_{LL} are not exactly known. Therefore a_{LL} has to be parametrized in terms of measured kinematic variables, in particular the transverse momentum of the D^0. This is done using a neural network which provides a 80% correlation between the generated and the reconstructed a_{LL}. The statistical gain due to including a_{LL} in the weight is particularly important since a_{LL} even changes sign within the acceptance. Finally the open-charm channel provides the preliminary result

$$\Delta G/G(x_g = 0.15, \mu^2 = 13 \text{ GeV}^2) = -0.57 \pm 0.41(stat) \pm 0.17(syst) \quad \text{(open charm)}. \qquad (1)$$

This is presented in Fig. 9 and compared to other results. The open-charm result still suffers from too low statistics.

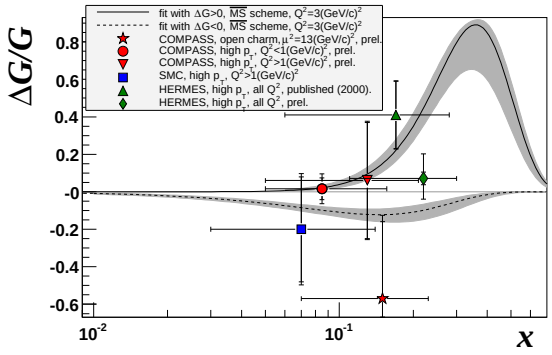

Figure 9. Results obtained by COMPASS for $\Delta G/G$ in the open-charm channel (★) and in the high p_t channel (● for $Q^2 < 1$ GeV^2 and ▼ for $Q^2 > 1$ GeV^2). These results are compared to measurements in the high p_t channel by SMC (■) [11] and HERMES (▲ and ♦) [12] and to the two solutions of our inclusive QCD analysis [2].

The physics backgrounds in the high-p_t-hadron pair channel include leading-order processes $\gamma^* q \to q$, where the p_t is provided by the fragmentation, QCD Compton processes, $\gamma^* q \to qg$, and the various "resolved-photon" processes where the virtual photon fluctuates to a hadronic states which then interacts with the nucleon. The latter represent more than half of the cross section at low Q^2 whereas they are practically negligible at $Q^2 > 1$ GeV^2.

The measured asymmetry can be written as $A_\parallel = R_{PGF} \times a_{LL} \times \frac{\Delta G}{G} + A_{bckg}$, where the fraction of PGF events, R_{PGF}, and the background asymmetry have to be estimated by MC. The analysis was performed separately for $Q^2 < 1$ and $Q^2 > 1$ GeV^2 samples. For the sample of events at $Q^2 < 1$ GeV^2, the PYTHIA event generator is used together with a GEANT simulation of the spectrometer. This provides a fair description of the experimental data as illustrated by Fig. 10. The $Q^2 > 1$ GeV^2 sample is analyzed in a similar way using the LEPTO event generator, but it provides ten times less statistics and is not discussed further here.

The dominant systematic error in the high p_t channel is due to the MC. It was estimated by varying the MC parameters in a range where the MC remains in reasonable agreement with the experimental data and looking at the largest variation of the resulting $\Delta G/G$. The most sensitive parameter is the intrinsic k_T inside the virtual photon. We get as a preliminary result [10]

$$\frac{\Delta G}{G}(x_g = 0.10, \mu^2 = 3 \text{ GeV}^2) = 0.016 \pm 0.058(stat) \pm 0.055(syst) \quad \text{(high } p_t\text{)}. \qquad (2)$$

The small systematic errors is due to the fact that it is largely proportional to the value of $\Delta G/G$. This result, presented on Fig. 9, disfavors models of $\Delta G(x)$ with a large value of the integral ΔG. In particular a value $\Delta G \approx 2 - 3$, which is needed if we want the axial anomaly to bring back $\Delta\Sigma$ to the expected value $\Delta\Sigma = a_8$, seem quite unlikely.

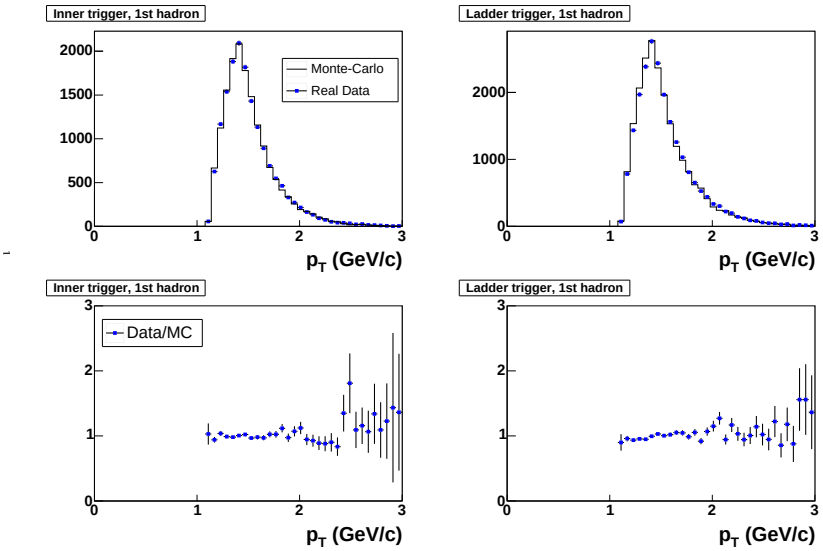

Figure 10. Upper plots: MC (——) and the real data (■) p_t distributions for two different triggers. lower plots: ratio of the two distributions.

6. Prospects and conclusions

All results presented here correspond to 2002-2004 data taking. An improved charm analysis is being developed by including a parametrization of the signal-to-background ratio in the event weight in order to gain some more statistics. There was no data taking in 2005. It resumed in 2006 with an improved set-up. The new PT magnet provides larger acceptance, the RICH detector was equipped with faster electronics and PMs in the inner region. The PT set-up was modified to include 3 target cells arranged in a way which largely cancels false asymmetries. Proton data (NH_3 target) were taken in 2007. They will provide the possibility of flavor separation in the semi-inclusive analysis.

The quark contribution to the nucleon spin is now well established to $\Delta\Sigma = 0.30 \pm 0.01 \pm 0.02$ since the error due to the low x contribution to Γ_1 has been strongly reduced and ΔG does not seem any more to be large enough to largely affect this result through the axial anomaly. The total valence contribution to the nucleon spin, $\Delta u_v + \Delta d_v = 0.41 \pm 0.07 \pm 0.05$, is two standard deviations below the expectation for a flavor symmetric sea and the data seem to indicate that $\Delta\bar{u} \approx -\Delta\bar{d}$. The fit to inclusive data gives two solutions with either sign of ΔG and an absolute value $|\Delta G| \approx 0.2 - 0.3$ while direct measurements of $\Delta G/G$ disfavor large values of ΔG. A value $\Delta G \approx 0.35$, giving $L_Z = 0$ is however still quite possible.

References

[1] COMPASS, Abbon P et al., 2007 *NIM* A **577** 455
[2] COMPASS, Alexakhin V et al., 2007 *Phys. Lett.* B **647** 330
[3] SMC, Adeva et al., 1998 *Phys. Rev.* D **58** 112001;
[4] HERMES, Airapetian et al., 2005 *Phys. Rev.* D **71** 012003;
[5] E143, Abe et al., 1998 *Phys. Rev.* D **58** 112003;
[6] E155, Anthony et al., 1999 *Phys. Lett.* B **463** 339;
[7] COMPASS, Alekseev M et al., Submitted to *Phys. lett.* B, hep-ex/0707.4077
[8] SMC, Adeva et al., 1998 *Phys. Lett.* B **420** 180;
[9] de Florian D, Navarro GA, Sassot R, 2005 *Phys. Rev.* D **71** 094018
[10] COMPASS 2002-2003 data: Ageev E et al., 2006 *Phys. lett.* B **633** 25
[11] SMC, Adeva et al., 2004 *Phys. Rev.* D **70** 012002
[12] HERMES, Airapetian et al., 2000 *Phys. Rev. lett.* **84** 2584